

A new method for the investigation of capillary structure

D.A. Tata^a, B.J. Anderson^{a,b,*}

^a Department of Psychology, State University of New York at Stony Brook, Stony Brook, New York, NY 11794-2500, USA

^b Program in Neurobiology and Behavior, State University of New York at Stony Brook, Stony Brook, New York, NY 11794-2500, USA

Received 19 July 2001; received in revised form 10 October 2001; accepted 10 October 2001

Abstract

Numerous physiological conditions as well as behavioral conditions have been shown to influence central nervous system vascular structure. Many of the methods used to investigate these structural alterations take advantage of the visibility of viscous substances (e.g. India ink in gelatin) perfused into the vasculature. The high viscosity of the solution, however, can cause incomplete vessel perfusion. The aim of the present study was to test whether or not capillaries seen in tissue perfused with fixative, embedded in celloidin and stained with Methylene Blue–Azure II ($n=6$) could be a useful alternative for the investigation of brain vascular structure. The method was compared to tissue from six rats perfused with India ink in gelatin and stained with cresyl violet. Qualitatively, vessels in the standard perfused tissue embedded in celloidin yielded clear vessels with stained pericytes. The two methods did not differ in branch point to cell ratio, length of individual capillaries, vessel length per mm³, and capillary tortuosity. The capillary diameter was greater in the celloidin embedded tissue than in the India ink perfused tissue. Measuring the diameter between vessel walls appears to provide a more accurate measure than the widest distance between India ink pigments. Quantitative comparisons suggest that perfusion with standard fixative followed by embedding in celloidin provides vascular quantification comparable to that from India ink perfused tissue. The present method has several advantages, which include visualization of pericytes, increased probability of complete perfusion, clear view of cells that might otherwise be obscured by opaque vessels, and the possibility of using the alternate cerebral hemisphere for investigation of vascular ultrastructure. © 2002 Elsevier Science B.V. All rights reserved.

Keywords: Vasculature; Blood vessels; India ink; Celloidin embedding; Capillary length; Capillary diameter; Tortuosity; Capillary morphology; Capillary geometry

1. Introduction

A main function of capillaries is to provide tissue oxygenation and to respond to changing oxygen demands (Pawlik et al., 1981; Hudetz et al., 1995; Hudetz, 1999). The study of microvascular geometry is of particular interest since it affects the oxygen supply (Chang et al., 1982; Hudetz et al., 1993; Pittman, 1995; Goldman and Popel, 2000). Capillary structural alterations in the central nervous system are now recognized to occur with neurodegenerative diseases (Berzin et al., 2000; Farkas et al., 2000), diabetes (Ward, 1993; Piotrowski et al., 1999), chronic hypertension (Farkas et al., 2000), and aging (Keuker et al., 2000). Changes also follow ischemia (Piotrowski et al., 1999), chronic hy-

poxia (Harik et al., 1995; Boero et al., 1999), chronic ethanol intoxication (Kraszpuski et al., 2000), chronic hypoperfusion (De Jong et al., 1999), and behavioral treatments (Sirevaag et al., 1988; Isaacs et al., 1992). Anatomical alterations of the vessels associated with the disease, insults and behavior occur at two levels. Ultrastructural changes in the vessel wall and basement membrane have been investigated using transmission electron microscopy (TEM) (De Jong et al., 1999; Piotrowski et al., 1999; Keuker et al., 2000), whereas alterations in vessel length per tissue volume (Boero et al., 1999), and capillary cross section density (Isaacs et al., 1992) have been studied at the light microscopic level of analysis.

A number of manipulations increase capillary density (Sirevaag et al., 1988; Isaacs et al., 1992; Boero et al., 1999). The exact mechanisms leading to changes in capillary density and vessel length per volume have not been investigated. Either existing vessels become more

* Corresponding author. Tel.: +1-631-632-7821; fax: +1-631-632-7876.

E-mail address: banderson@notes.cc.sunysb.edu (B.J. Anderson).

tortuous, with greater length between existing branch points, or new vessels are added. The latter would require the addition of branch points so that branch point density per cell would increase. The two alternatives would have different implications for local cerebral blood flow (Motti et al., 1986). Here we use a microscope tracing system to carry out methods that will allow the quantification of capillary length and diameter, tortuosity and branch point density. Visualization of capillary geometry in three dimensions at the light microscopic level of analysis has typically utilized perfusion of the vascular lumen with various substances, including microfil, color opaque gelatins, and India ink (Broadwell et al., 1987). The intravascular injection of India ink is a widely used method for the quantification of the vascular network (Lawrence et al., 1984; Sirevaag et al., 1988; Finger and Dunnett, 1989; Korol and Brunjes, 1992; Miyoshi et al., 1995). Typically brains are perfused with buffer followed by a solution of India ink and gelatin in buffer (Sirevaag et al., 1988). Brains are post-fixed and frozen prior to sectioning. The India ink perfusion method allows the use of unbiased sampling schemes and methods in the region of interest. Unfortunately, it has been criticized for its potential to produce artifacts attributed to incomplete perfusion (Broadwell et al., 1987), ruptured vessels (Korol and Brunjes, 1992), or a disrupted view of vessels when the network is very dense (Duvernoy et al., 1981, 1983).

An ideal method for quantifying structural features of brain vasculature in an experimental context should include complete visualization of the capillary network, an unobstructed view of cells, and complete perfusion. An ideal method would reduce variance reflecting animal differences and variability in the region of interest by providing efficient methods of data collection so that a sufficient number of animals and sample sites within the region of interest can be used (Gundersen et al., 1988). Last, an ideal method would allow the use of a standard fixative so that the opposite hemisphere would be available for ultrastructural analysis.

We present a novel use for a standard histological procedure. Vessels can be visualized in tissue perfused with standard fixative and embedded in celloidin (Fig. 2). To determine whether or not celloidin embedded tissue could be a useful alternative for the measurement of three-dimensional vasculature, we quantified vascular structural characteristics in celloidin embedded tissue and compared it to estimates from India ink perfused tissue. Branch points per neuron, capillary length, tortuosity and diameter measurements were collected in tissue perfused with India ink and frozen, and in tissue perfused with standard fixative and embedded in celloidin. All data were collected with the optical disector combined with a representative random sampling scheme within the region of interest in each

section. The region of interest was hind limb representations of layer 2/3 of the motor cortex within four comparable coronal sections (Paxinos and Watson, 1986). If the celloidin method is comparable to the India ink perfusion technique within these comparable areas, then it will provide the opportunity to collect representative random sampling in any region of interest without the disadvantages associated with the ink perfusion method.

2. Methods

2.1. *Animals and tissue preparation*

Twelve Long Evans Hooded female rats (Simonsen stock) aged 7–9.5 months old were anesthetized with ketamine (120 mg/kg) and xylazine (13 mg/kg). Six randomly chosen rats were intracardially perfused with 0.1 M phosphate buffer (PB) followed by 6% gelatin and 25% India ink in 0.1 M PB (Sirevaag et al., 1988). Brains were post-fixed in sucrose formalin and sectioned frozen with a sliding microtome at 108 μm thickness. They were then stained with a standard protocol for cresyl violet. Six rats were intracardially perfused with Tyrode's solution followed by 2% paraformaldehyde and 2.5% glutaraldehyde in 0.1 M PB. Brains were dehydrated and infiltrated with celloidin as described by Glaser and Van der Loos (1981), with the exception of Parlodian concentrations. Brains were infiltrated with 5.3% Parlodian followed by infiltration and embedding in 10.6% Parlodian. Thick sections (30 μm) were collected in butanol, passed through a series of reduced alcohol concentrations, placed in 0.1 M PB for 5 min followed by 1% periodic acid in 0.1 M PB for 5 min. Sections were then stained in a mixture of 0.16% Methylene Blue, 0.1% Azure II, 1.7% Na_2HPO_4 and 0.56% KH_2PO_4 for 3–10 min. After staining, sections were rinsed in 0.1 M PB for 5 min, dehydrated in 50% EtOH for 2 min, then differentiated in 70% EtOH with five drops of glacial acetic acid for 15–20 min followed by dehydration and coverslipping.

2.2. *Sampling methods and quantification*

2.2.1. *Sampling area*

In order to compare measures from the two methods, we chose four identical coronal planes (–2.8, –2.3, –1.8, and –0.8 mm from bregma). Measurements were taken from layer two and three of the hind limb representations of the motor cortex equivalent to the location of hind limb representations in Paxinos and Watson (1986). These regions were defined by subcortical landmarks. Data were collected with a Zeiss Axio-plan 2 light microscope and sampling sites (optical

disectors) of known volume and even distribution over the region of interest were identified by using the optical fractionator probe provided by the STEREO INVESTIGATOR software (MicroBrightField, Inc., Colchester, VT, Version 2000). Within each of the pre-selected sections, this probe generated uniformly random sample sites over the region of interest. The dimensions of the sampling sites and their distribution for density measures were determined by first collecting pilot data to calculate the parameters needed to keep the coefficient of variation lower than 10%. The distance between the counting frames in the xy plane (scan grid size) was 80 μm . The length and width of the counting frame (optical disector) was 50 μm for both celloidin embedded and frozen India ink tissue for branch point density data, 30 μm for cell density and 80 μm for capillary length and diameter measurements. The height of a counting frame, the distance between the top and bottom of the disector optical planes within the section, was set at 15 μm for the celloidin embedded tissue and 20 μm for the frozen India ink tissue. The height of the counting frame is not equal to the section thickness allowing for the existence of upper and lower guard zones. Guard zones avoid problems associated with the counting particles that have been truncated at the surface of the sections (lost caps) (Sterio, 1984; Gundersen, 1986; West et al., 1991; Hedreen, 1998). The upper guard zone was always 5 μm thick and the lower was at least 5 μm thick.

2.3. Section thickness

The section thickness, t , is necessary for determining the height of the counting frame and its guard zone. Since many histological processes cause shrinkage of the tissue in the z -axis, the true physical section height has to be estimated. For this purpose, the thickness was measured at five points (selected with a uniform random systematic sampling scheme within sections) with the use of an immersion oil objective and a z -axis microcator. The section thickness was the average of these five measurements. Two sets of thickness measurements were taken for each section.

2.4. Parameters for measurements

A 100 \times oil objective with high numerical aperture (1.4) was used to measure capillary diameter, branch point density, cell density and vessel length. The optical disector counting rules were applied to ensure unbiased counting (Sterio, 1984). Sampling grids on a miniature high-resolution monitor (Lucivid, Microbrightfield Inc., Colchester, VT) were projected into the microscopic image through the drawing tube port so that data could be collected directly from the optical image.

2.5. Correction for shrinkage

Because of the shrinkage of the frozen India ink sections in the z -axis and the celloidin standard perfusate sections in the x , y , and z -axes, shrinkage correction was required. The STEREO INVESTIGATOR software allows the adjustment of the measurements by entering the appropriate correction factor for each axis. The correction factor for the India ink tissue was 2.0725 (z -axis or anterior–posterior axis), which is equal to the ratio of thickness in which the tissue was cut (108 μm) over the mean thickness after mounting onto the slides and dehydration (52.11 μm). Our estimates for z -axis shrinkage in frozen sections are similar to a previous report (Messina et al., 2000). In order to estimate the shrinkage correction factor in the z -axis for celloidin embedded tissue, we used data from another experiment conducted in the lab (unpublished data). In that experiment, caliper measurements of the brain in all three axes were taken after extraction, before dehydration, and after embedding tissue in celloidin. After embedding, shrinkage was uniform in x and y -axes (original/embedded: 1.14), in contrast to the z -axis where the shrinkage was less (original/embedded: 1.05). To normalize celloidin embedded tissue to India ink perfused tissue, the square root of the ratio of the mean coronal area of India ink sections over the mean coronal area of the celloidin tissue, after excluding the ventricular areas, was calculated to obtain a final correction factor of 1.195. For the z -axis, we adjusted the final x and y correction factor (1.195) to take into account the lower shrinkage in the z -axis (original/embedded: 1.05) to obtain a correction factor of 1.10.

2.6. Ratio of branch point density to neuron density

The number of branch points per neuron was calculated as the ratio of branch point density to neuron density. The number of branch points and neuronal nuclei were estimated with the disector method (Sterio, 1984). The particles (branch points, neurons) that came into focus within the counting frame, as it was moved through a known distance of section thickness (height of the disector), constituted the number of branch points or neurons (Q^-) contained in one optical disector. In the celloidin embedded tissue stained with Methylene Blue–Azure II, neurons were differentiated from glial cell on the basis of their prominent, dark nucleolus, large spherical nucleus and a clear nuclear membrane (Ling et al., 1973). In India ink perfused tissue that was frozen and stained with cresyl violet, neurons were differentiated from glial cells by their triangular shape and the presence of axon hillock as well as by the absence of chromatin masses. The density of the branch points and neurons in each section was equal to the sum of Q^- over the total volume of the optical disec-

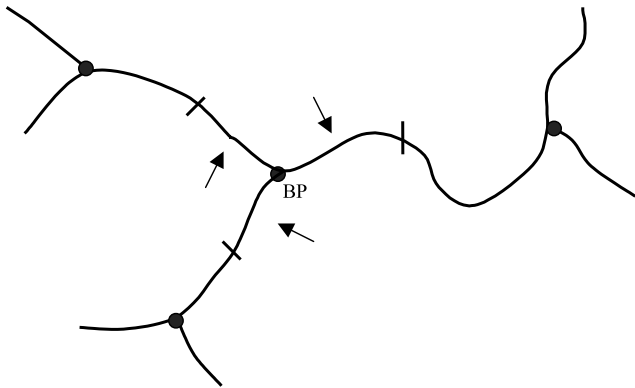
tors (volume of each counting frame multiplied by the total number of counting frames) of the section. The branch point and cell density for each animal was the grand mean for the four sections.

2.7. Vessel length, tortuosity and diameter

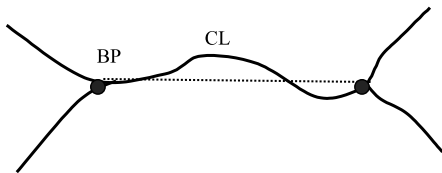
Inner (luminal) capillary diameter measurements, taken in the x and y -axes only, were estimated by measuring the inner diameter (celloidin) or the diameter of the India ink opacity perpendicular to the vessel axis (Fig. 1C). Diameter measurements in the celloidin standard perfusate were corrected for shrinkage in x and y -axes relative to the India ink perfused tissue. The upper limit for capillary profiles was $10\ \mu\text{m}$ (Bar, 1980). Three or four measurements were taken depending on the length of the segment. Both the length of the

capillaries and the shortest distance between the two branch points were measured. These measurements were taken in the x , y and z -axes, and were corrected for shrinkage in all the three axes. Tortuosity of the capillaries was calculated as the ratio of capillary length to the shortest distance between the two branch points (Fig. 1B). These measures were first averaged within each coronal plane. A grand mean was then computed for the averages taken from each of the four coronal planes. Total vessel length per mm^3 was also calculated. Since each branch point is the junction for three vessels (Fig. 1A), each branch point is proportional to half of three segments, or 1.5 vessel segments. Consequently, the total capillary length per mm^3 would be equal to (branch point density $\times 1.5$) \times segment length (μm). This method of calculating capillary length in a volume of tissue takes advantage of the capillary length measurements in the z -axis obtained with the STEREO INVESTIGATOR software, as well as the length in the x and y -axes.

A



B



C

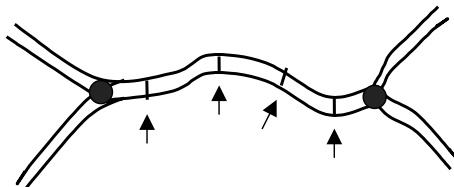


Fig. 1. (A) Branch point (BP) is the junction for three vessels. Consequently, each branch point is proportional to half of three capillaries, which equals 1.5 vessel segments (arrows) per branch point. (B) Tortuosity of capillaries was calculated as the ratio of capillary length (CL) to the shortest distance (SD) between branch points. (C) Three or four lines were drawn perpendicular to the capillary axis, depending on the length, and averaged for an estimate of capillary diameter.

3. Results

3.1. Ratio of branch point density to neuron density

The number of branch points per neuron in the celloidin standard perfusate tissue ($M = 0.0474$, $SE = 0.0027$) was not significantly different from the ratio estimated in frozen India ink tissue ($M = 0.0566$, $SE = 0.0071$), [$t(10) = -1.201$, $P = 0.257$; Fig. 3].

3.2. Capillary segment length

The range of animal means for segment length was $32.206\text{--}51.207\ \mu\text{m}$ for celloidin standard perfusate tissue and $42.496\text{--}51.636\ \mu\text{m}$ for frozen India ink tissue. A t -test for independent samples revealed a non-significant difference between the two groups, [$t(10) = -1.693$, $P = 0.121$; Fig. 4].

3.3. Total vessel length per mm^3

Total vessel length [branch point density $\times 1.5$ (number of segments per branch point) \times segment length] for celloidin standard perfusate tissue was $303\ \text{mm}/\text{mm}^3$ of tissue, whereas total capillary length in frozen India ink tissue was estimated to be $215\ \text{mm}/\text{mm}^3$ of tissue. The difference was non-significant between the two groups, [$t(10) = 2.086$, $P = 0.064$; Fig. 5].

3.4. Capillary tortuosity

A t -test for independent samples revealed a trend for differences in tortuosity of capillary segments, [$t(10) = -2.215$, $P = 0.051$]. The capillaries of the frozen India

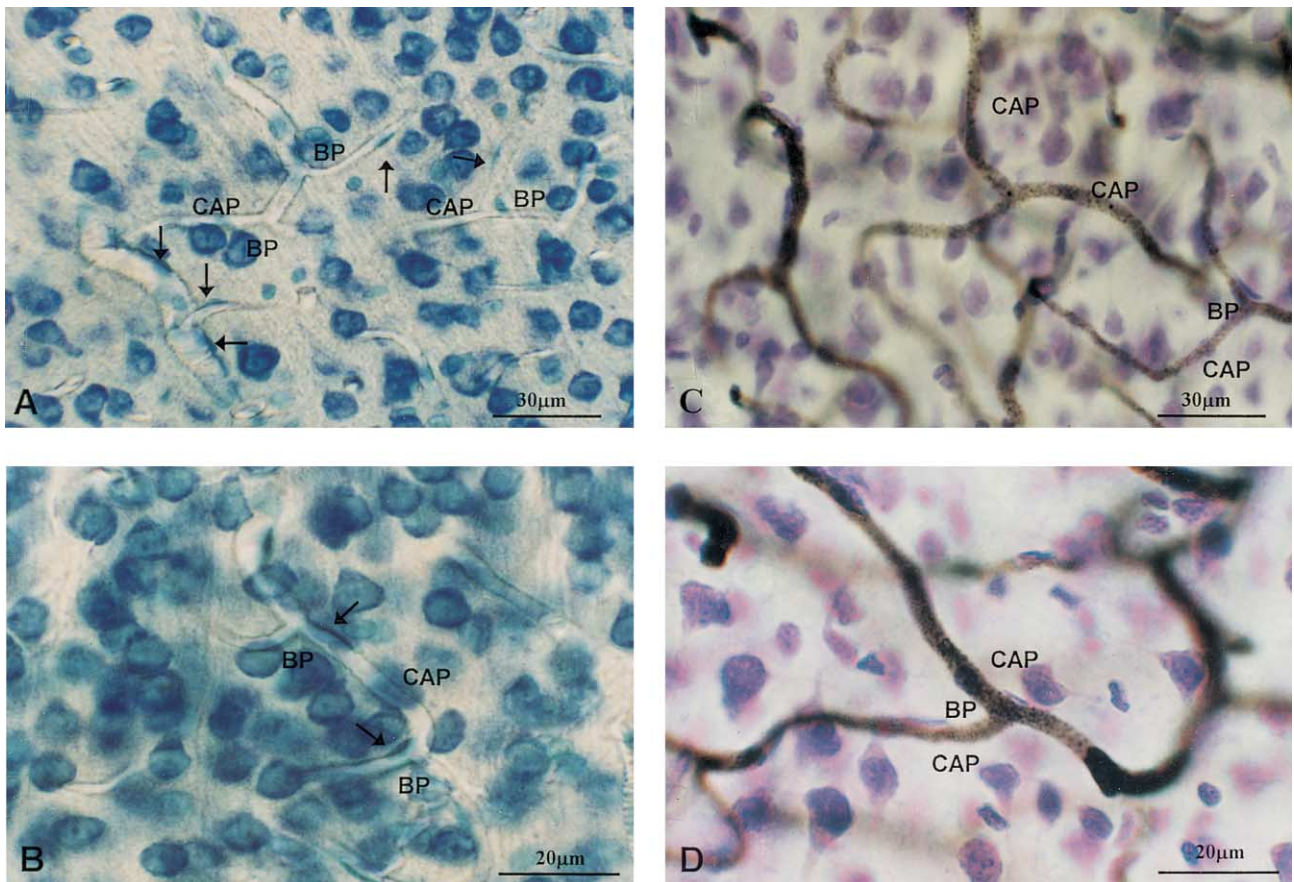


Fig. 2. In celloidin standard perfusate tissue (A and B), light diffraction provides a clear view of capillaries segments (CAP) and branch points (BP) tissue despite their transparency. The visibility of the capillary walls (arrow) allows the accurate estimation of the diameter. Pericytes can also be visualized with the Methylene Blue–Azure II stain (arrows). (C and D) Capillaries (CAP) perfused with India ink. In frozen India ink tissue the capillary walls are not visible. Consequently, the diameter was a direct measure of the width of the ink in the vessel. A and C: bar = 30 μm, B and D: bar = 20 μm.

ink tissue ($M = 1.197$, $SE = 0.016$) tended to have greater tortuosity than those of the celloidin standard perfusate tissue ($M = 1.132$, $SE = 0.024$; Fig. 6).

3.5. Capillary diameter

The capillary diameters from the raw data ranged from 1.692 to 9.662 μm for the celloidin standard perfusate and 1.708 to 9.626 μm for the frozen India ink tissue. The vessels of celloidin standard perfusate tissue ($M = 3.986$, $SE = 0.101$) had larger diameters compared to the frozen India ink capillaries ($M = 3.477$, $SE = 0.088$) [$t(10) = 3.479$, $P = 0.006$; Figs. 2 and 7).

3.6. Variance of section thickness

The mean uncorrected section thickness per group was estimated by averaging the mean thickness of all the six animals, and was equal to 31.35 and 52.11 μm for the celloidin embedded and India ink tissue, respectively. During counting, it was noticed that the five

measurements for each section tended to be more variable in the India ink tissue compared to the celloidin tissue. A one-way ANOVA on the mean difference between the maximum and minimum values for each of the four sections revealed a significant effect of group [$F(1,10) = 5.607$, $P < 0.05$], with India ink having more variability.

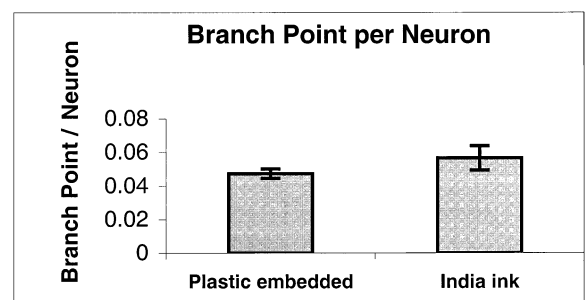


Fig. 3. Ratio of branch point density to neuron density. The number of capillary branch points per neuron did not differ between the celloidin standard perfusate tissue and the frozen India ink tissue. Bars are means \pm SEM.

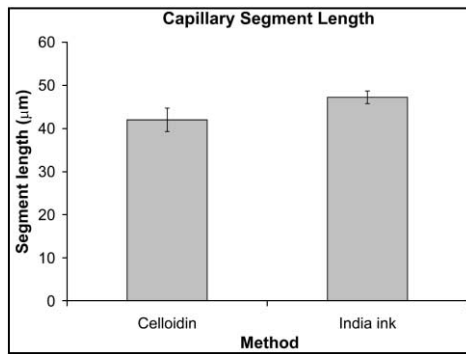


Fig. 4. Individual capillary segment length in micrometer. No significant difference was found for vessel segment length. Bars are means \pm SEM.

4. Discussion

The aim of this study was to test whether or not tissue perfused with standard fixative and embedded in celloidin can be used for the accurate investigation of vascular structure. More specifically, we have attempted to establish that celloidin embedded, aldehyde-fixed, Nissl-impregnated tissue provides the opportunity to quantify capillaries, which are visible because of light diffraction. Therefore, we have compared this method against the India ink perfusion method, which has been one popular approach to vascular quantification. There was no difference between the two methods in the ratio of branch point/neuron, capillary segment length, or total capillary length per mm^3 .

Branch points are clearly visible in India ink perfused tissue, but are less clear in tissue embedded in celloidin. This qualitative difference did not appear to influence the ability to identify the branch points because there was no difference in branch point/neuron density between the two methods. Thus, the data indicate that capillaries in celloidin embedded tissue were as visible as those in the frozen India ink tissue.

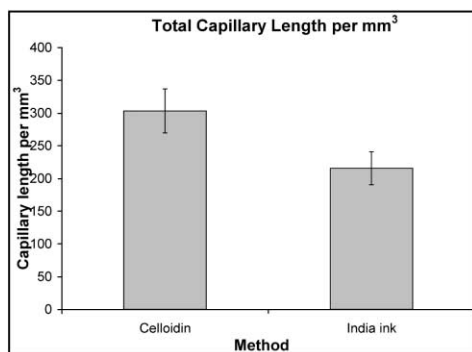


Fig. 5. Total capillary length per mm^3 . The total vessel length per mm^3 was not significantly different between the two methods. Bars are means \pm SEM.

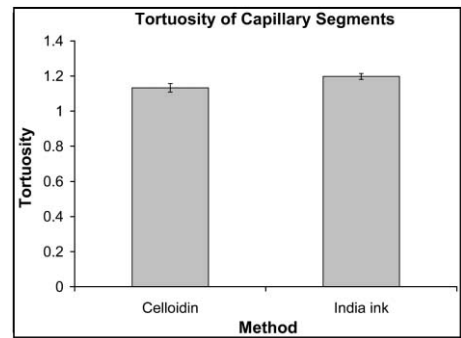


Fig. 6. Tortuosity of capillary segments. The ratio for vessel length between branch points to shortest distance between branch points tended to be greater in the India ink perfused tissue relative to the celloidin standard perfusate tissue. Bars are means \pm SEM.

The capillary segment length and total capillary length per mm^3 were two other geometric characteristics that did not significantly differ between the celloidin standard perfusate tissue and frozen India ink tissue. However, there was a trend for the total capillary length per mm^3 to be longer in the celloidin embedded tissue. As mentioned in Section 3.3 the estimation of this variable was a function of the branch point density, segment length and the number of segments per branch point. We suspect that the trend for greater capillary length per mm^3 partially reflects the higher branch point density in the celloidin embedded tissue relative to the India ink perfused tissue (data not shown).

While there was not a significant difference in tortuosity between the two groups, there was a trend for the capillaries of the frozen India ink tissue to be more tortuous than the vessels of celloidin standard perfusate tissue. The source of this difference is unclear. We question whether the substantial shrinkage in the z -axis of the frozen India ink tissue influences the tortuosity estimate. Although there is also shrinkage of the celloidin embedded tissue, the shrinkage is more uniform across axes.

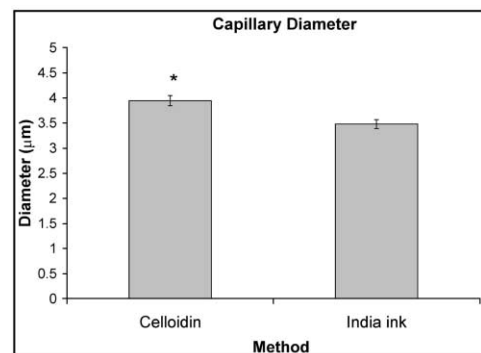


Fig. 7. Diameter of capillary segment. The capillaries of celloidin standard perfusate tissue had larger diameters compared to the India ink capillaries. Bars are means \pm SEM. * = $P < 0.05$.

Diameter of vessel segments was larger in celloidin standard perfusate tissue relative to the diameter measured in the frozen India ink tissue. We suspect that this result reflects a difference in the methodology rather than true vessel diameter. In the India ink perfused tissue the diameter was a direct measure of the projected diameter. In both tissues the inner diameter was measured. However, since the perfusate was a 25% solution of ink, we suspect that ink may not have extended the full distance across the capillary lumen. In contrast, in celloidin standard perfusate tissue the diameter measurements were based on the distance between the two visible vessel walls. Since only the luminal diameter was measured in celloidin tissue, the greater capillary diameter in celloidin embedded tissue cannot be attributed to the measurement of the endothelium. The variability in celloidin embedded tissue was very low.

All variables that were estimated by direct measurements (e.g. capillary segment length, and diameter) had very low standard error of the mean (SEM). The SEM for capillary segment length was between 5 and 11%. For diameter measures, the SEM was within 2.5% of the mean for each group. Similarly, tortuosity, which reflected capillary segment length over the shortest distance between two branch points, also had very low SEM, within 1–2% of the mean. When measures were combined to produce branch point density per neuron and total capillary length per mm³ the error rates were higher. For branch point density per neuron the SEM from celloidin embedded tissue was lower (5%) than from the India ink perfused tissue (13%). We suspect that the neuron density measures from celloidin embedded tissue were less variable because neurons were more easily distinguishable from glial cells than in frozen tissue. Total capillary length per mm³ is the product of capillary segment length multiplied by the branch point density. The relatively larger variability in this measure is likely to reflect the combined variance across the two measures, SEM being between 11 (celloidin embedded) and 12% (India ink) of the mean. When estimates are to be combined it may be important to increase the sample size in order to reduce the error.

We chose not to use the cycloid method (Baddeley et al., 1986; Gundersen et al., 1988), which is a popular and efficient sampling method for estimating the surface density. Although surface density reflects two variables of interest, capillary length and diameter, the cycloid method requires that the area of interest be dissected from the tissue section and randomly rotated around a vertical axis. Our measurement of vessel length by tracing vessel segments in three dimensions provides the opportunity to keep the region of interest intact within the original section so that the mapping of the region can take place after coverslipping. This improves the accuracy of mapping, especially when

borders are subtle. When investigators have a region of interest with obvious borders the cycloid method may be more efficient. When vertical sections can be obtained so that Sv is estimated with the cycloid method, tortuosity can be calculated as the ratio of surface density to branch point density (Sv/BPv).

Because standard perfusate is used with celloidin embedding, this method also provides the capability of harvesting tissue for both light and electron microscopic investigation. Tissue to be used for electron microscopy could be obtained from the region of interest dissected from one hemisphere and embedded in epoxy, while branch points/neuron, capillaries length, and capillary diameter measures could be quantified from the alternate hemisphere embedded in celloidin. This may be particularly useful for investigators who wish to study vascular alterations at both the cellular and ultrastructural level of analysis. For example, endothelial cell thickness could be estimated in EM embedded tissue. The data collection methods used here, and the measures reported, offer an opportunity to clarify the morphological changes that lead to changes in capillary density and vessel length per volume following conditions such as hypoxia (Boero et al., 1999), exercise (Isaacs et al., 1992) and housing in an enriched environment (Sirevaag et al., 1988).

In conclusion, the findings that branch point/neuron, capillary segment length, and total length per mm³ did not significantly differ support our initial hypothesis that tissue perfused with standard perfusate and embedded in celloidin can be used to quantify vascular structure in a manner comparable to that achievable with India ink perfusion. In the present study the estimation of the volume of the area of interest was not necessary. It should be noted, however, that when the celloidin method is used across conditions that may change the cell number and tissue volume, the estimation of the reference volume is necessary. The visualization of the capillaries allows the identification of branch points and the quantification of other morphological characteristics (length, tortuosity, diameter) of capillaries. Based on our qualitative observations, vessels perfused with India ink obstruct the view of cells beneath them, thereby underestimating cell density. In contrast, the translucence of the vessel lumen in celloidin embedded tissue provides a view of cell bodies below the vessel. The Methylene Blue–Azure II stain adds the advantage of visualizing pericytes, which may be of interest to many investigators. The present method may not be superior to methods that include complete reconstruction from semi-thin sections (Davies et al., 1996), but it provides a means for efficient sampling within an experimental context. We have found that the strengths of the celloidin embedding method over the India ink perfusion method include increased probability of complete perfusion, clear view of cells that may otherwise

be obscured by opaque vessels, quantification of morphological characteristics, use of automated tracing systems, and the capability for unbiased representative sampling.

Acknowledgements

This work was supported by the National Institute of Mental Health Grants MH62075.

References

- Baddeley AJ, Gundersen HJG, Cruz-Orive LM. Estimation of surface area from vertical sections. *J Microsc* 1986;142(3):259–76.
- Bar T. The vascular system of the cerebral cortex. Berlin: Springer, 1980:63.
- Berzin TM, Zipser BD, Rafii MS, Kuo-Leblanc V, Yancopoulos GD, Glass DJ, et al. Agrin and microvascular damage in Alzheimer's disease. *Neurobiol Aging* 2000;21(2):349–55.
- Boero JA, Jonathan A, Arregui A, Rovainen C, Woolsey TA. Increased brain capillaries in chronic hypoxia. *J Appl Physiol* 1999;86(4):1211–9.
- Broadwell RD, Charlton HM, Balin BJ, Salzman M. Angioarchitecture of the CNS, pituitary gland, and intracerebral grafts revealed with peroxidase cytochemistry. *J Comp Neurol* 1987;260:47–62.
- Chang BL, Takashi Y, Nuccio J, Pace R, Bing R. Microcirculation of left atrial muscle cerebral cortex and mesentery of the cat. *Circ Res* 1982;50:240–9.
- Davies KR, Richardson G, Akmentin W, Acuff V, Festermacher JD. The microarchitecture of cerebral vessels. In: Couraud, Scherman, editors. *Biology and physiology of the blood–brain barrier*. New York: Plenum Press, 1996:83–91.
- De Jong GI, Farkas E, Stienstra CM, Plass JR, Keijsers JN, de la Torre JC, et al. Cerebral hypoperfusion yields capillary damage in the hippocampal CA1 area that correlates with spatial memory impairment. *Neuroscience* 1999;91(1):203–10.
- Duvernoy H, Delon S, Vannson JL. Cortical blood vessels of the human brain. *Brain Res Bull* 1981;7:519–79.
- Duvernoy H, Delon S, Vannson JL. The vascularization of the human cerebellar cortex. *Brain Res Bull* 1983;11:419–80.
- Farkas E, De Jong GI, Apro E, De Vos RA, Steur EN, Luiten PG. Similar ultrastructural breakdown of cerebrocortical capillaries in Alzheimer's disease, Parkinson's disease, and experimental hypertension. What is the functional link? *Ann N Y Acad Sci* 2000;903:72–82.
- Finger S, Dunnett BS. Nimodipine enhances growth and vascularization of neural grafts. *Exp Neurol* 1989;104:1–9.
- Glaser EM, Van der Loos. Analysis of thick brain sections by obverse–reverse computer microscopy: application of a new, high clarity Golgi–Nissl stain. *J Neurosci Methods* 1981;4(2):117–25.
- Goldman D, Popel AS. A computational study of the effect of capillary network anastomoses and tortuosity on oxygen transport. *J Theor Biol* 2000;206(2):181–94.
- Gundersen HJG. Stereology of arbitrary particles. A review of unbiased number and size estimators and the presentation of some new ones, in memory of William R. Thompson. *J Microsc* 1986;143:3–45.
- Gundersen HJG, Bendtsen TF, Korbo L, Marcussen N, Moller A, Nielsen K, et al. Some new, simple and efficient stereological methods and their use in pathological research and diagnosis. *APMIS* 1988;96:379–94.
- Harik SI, Hritz MA, LaManna JC. Hypoxia-induced angiogenesis in the adult rat. *J Physiol* 1995;485(Pt 2):525–30.
- Hedreen JC. Lost caps in histological counting methods. *Anat Rec* 1998;250(3):366–72.
- Hudetz AG. Mathematical model of oxygen transport in the cerebral cortex. *Brain Res* 1999;817(1–2):75–83.
- Hudetz AG, Feher G, Weigle CG, Knuese DE, Kampine JP. Video microscopy of cerebrocortical capillary flow: response to hypotension and intracranial hypertension. *Am J Physiol* 1995;268(6 Pt 2):H2202–10.
- Hudetz AG, Greene AS, Feher G, Knuese DE, Cowley AW Jr. Imaging system for three-dimensional mapping of cerebrocortical capillary networks in vivo. *Microvasc Res* 1993;46(3):293–309.
- Isaacs KR, Anderson BJ, Alcantara AA, Black JE, Greenough WT. Exercise and the brain: angiogenesis in the adult rat cerebellum after vigorous physical activity and motor skill learning. *J Cereb Blood Flow Metab* 1992;12:110–9.
- Keuker JI, Luiten PG, Fuchs E. Capillary changes in hippocampal CA1 and CA3 area of the aging rhesus monkey. *Acta Neuropathol (Berl)* 2000;100(6):665–72.
- Korol DL, Brunjes PC. Unilateral naris closure and vascular development in the rat olfactory bulb. *Neuroscience* 1992;46:631–41.
- Kraszpulski M, Tukaj C, Wrzolkowa T. Hippocampal capillaries in different age groups of chronically ethanol-intoxicated rats. *Morphometrical Stud* 2000;59(2):121–9.
- Lawrence JM, Huang SK, Raisman G. Vascular and astrocytic reactions during establishment of hippocampal transplants in adult host brain. *Neuroscience* 1984;12(3):745–60.
- Ling EA, Paterson JA, Privat A, Mori S, Leblond CP. Investigation of glial cells in semithin sections. I. Identification of glial cells in the brain of young rats. *J Comp Neurol* 1973;149(1):43–71.
- Messina A, Sangster CLC, Morrison WA, Galea MP. Requirements for obtaining unbiased estimates of neuronal numbers in frozen sections. *J Neurosci Methods* 2000;97:133–7.
- Miyoshi Y, Date I, Ohmoto T. Three-dimensional morphological study of microvascular regeneration in cavity wall of the rat cerebral cortex using the scanning electron microscope: implications for delayed neural grafting into brain cavities. *Exp Neurol* 1995;131:69–82.
- Motti E, Imhof H, Yasargil M. The terminal vascular bed in the superficial cortex of the rat. An SEM study of corrosion casts. *J Neurosurg* 1986;65:834–56.
- Paxinos G, Watson C. *The rat brain in stereotaxic coordinates*, 2nd ed. San Diego, CA: Academic Press, 1986.
- Pawlik G, Rackl A, Bing R. The quantitative capillary topography and blood flow in the cerebral cortex of cats: an in vivo microscopic study. *Brain Res* 1981;208(1):35–58.
- Piotrowski P, Gajkowsak B, Olszewska H, Smialek M. Electron microscopy studies on experimental diabetes and cerebral ischemia in the rat brain. *Folia Neuropathol* 1999;37(4):256–63.
- Pittman RN. Influence of microvascular architecture on oxygen exchange in skeletal muscle. *Microcirculation* 1995;2(1):1–18.
- Sirevaag AM, Black JE, Shafron D, Greenough WT. Direct evidence that complex experience increases capillary branching and surface area in visual cortex of young rats. *Brain Res* 1988;471(2):299–304.
- Sterio DC. The unbiased estimation of number and sizes of arbitrary particles using the disector. *J Microsc* 1984;134(2):127–36.
- Ward JD. Abnormal microvasculature in diabetic neuropathy. *Eye* 1993;7(2):223–6.
- West MJ, Slomianka L, Gundersen HJ. Unbiased stereological estimation of the total number of neurons in the subdivisions of the rat hippocampus using the optical fractionator. *Anat Rec* 1991;231(4):482–97.